UNIZIK JOURNAL OF ENGINEERING AND APPLIED SCIENCES (UJEAS)

Research Article

Examining the Kinetics and Thermodynamics of Chlorpyrifos Adsorption unto Activated Mucuna pruriens Seed Shell

Chukwudi Nkiruka Florencea, Igwegbe Chinenye Adaobia, Obiora-Okafo Ifeoma Amaoge, Nweke Chinenyenwa Nkeiruka.

Special Issue
A Themed Issue in Honour of Professor Onukwuli Okechukwu Dominic (FAS).

This special issue is dedicated to Professor Onukwuli Okechukwu Dominic (FAS), marking his retirement and celebrating a remarkable career. His legacy of exemplary scholarship, mentorship, and commitment to advancing knowledge is commemorated in this collection of works.

Edited by
Chinonso Hubert Achebe PhD.
Christian Emeka Okafor PhD.

UJEAS

UNIZIK JOURNAL OF ENGINEERING AND APPLIED SCIENCES

UNIZIK Journal of Engineering and Applied Sciences 4(1), March (2025), 1631-1646
Journal homepage: https://journals.unizik.edu.ng/index.php/ujeas
PRINT ISSN: 2992-4383 || ONLINE ISSN: 2992-4391

Examining the Kinetics and Thermodynamics of Chlorpyrifos Adsorption unto Activated *Mucuna pruriens* Seed Shell

Chukwudi Nkiruka Florence, Igwegbe Chinenye Adaobi, Obiora-Okafo Ifeoma Amaoge *, Nweke Chinenyenwa Nkeiruka

Chemical Engineering Department, Nnamdi Azikiwe University, Awka
*Corresponding Author's E-mail: nf.chukwudi@unizik.edu.ng

Abstract
The excessive use of pesticides (chlorpyrifos) in modern agriculture has increased chlorpyrifos in water. Hence, there is a need for imperative attention on alleviation of the negative impacts**.** This study evaluated the possible use of *Mucuna pruriens* seed shell (MPSS) as a bio-sorbent. MPSS was treated and activated by adding 1M of H_3PO_4, characterized using Fourier transform infrared spectroscopy (FTIR), scanning electron microscope-Energy dispersive X-ray (SEM-EDX) and Brunaer-emmett-teller (BET). The maximum efficiency of CLPF adsorption onto MPSS was 94.43% at optimum conditions of 30 mg/l adsorbate concentration, pH 6, and MPSS dosage of 0.5g/100ml. From the Isotherm results, all the models except Halsey describe the system well, but Temkin at 30 ^oC produced the best fit, with the highest correlation, R^2 of 0.9995 with the amounts adsorbed at 30, 35 and 40 ^oC to be 11.75 mg g^{-1}, 30.90 mg g^{-1} and 51.29 mgg^{-1} respectively. Pseudo second-order best described the kinetics study with the R^2 value of 0.9987. Thermodynamic parameters of ΔH^0, ΔS^0 and ΔG^0 values at optimum temperature (40^oC) were -0.008 KJ/mol, -0.441 KJ/Kmol and +0.134 KJ/mol respectively. The adsorption process was practicable and accepted with cation exchange between the adsorbate and adsorbent as the rate-limiting phase. Experimental results illustrate that adsorption capacity increased with pH, sorbent dosage and concentration. Conclusively, MPSS is an efficient adsorbent for removing chlorpyrifos.

Keywords: Chlorpyrifos, Mucuna Pruriens Seed Shell (MPSS), Adsorption isotherm, Kinetics, Thermodynamics

1. Introduction

Chlorpyrifos (O, O–diethyl–O–3,5,6–trichloro–2-pyridylthioate) ($C_9H_{11}Cl_3NO_3PS$) is an organophosphorus pesticide (OPP), colorless to white crystal solid, with mild mercaptan (thiol) odour, and having a similar smell with sulfur, is a widely used active insecticide that is effective by ingestion and contact (Zalat *et al.*, 2014). Chlorpyrifos is usually mixed with oily liquid before being used in crops and animals but is more complex when combined with other pesticides, which might result to serious toxic formulation (Iwuozor *et al.*, 2023, Rahamani *et al.,2021*). Today, chlorpyrifos has been reported to be used unchecked in excess all over the world causing high contaminations of a lot of natural elements (Joshi *et al*., 2023; Iwuozor *et al.*, 2023; Igwe *et al.*, 2018). For these reasons, research has been conducted to provide a low-cost method to mitigate their side effects.

The treatment technologies that have been in use for a long in the conduct of pollutants in wastewater generally include; photocatalytic procedures, nano-separation, membrane bioreactor and galvanized mud. Although new advanced technologies are emerging such as: biochar, microalgae, bioremediation, precipitation, ion exchange, chemical oxidation and adsorption method and many more (Nitin *et al.*, 2023).

In the present time, agricultural by-products, waste materials have become a very rich sources of workable adsorbents (Obiora-Okafo and Onukwuli, 2018; Dai *et al*. 2018; Saga and Samaka 2021). They are very helpful over synthetic adsorbents since they are readily available, economic, environmentally friendly, decayable and cost-effective (Kyzas and Kostoglou 2014; Omo-Okoro *et al*., 2018). Among the commonly used biomass as adsorbents by many researchers includes: peelings, rinds, stocks, starch, fibre, leaves, corks, shells, etc. They are natural equipment with good

adsorption potential (Ighalo *et al., 2020a*). This study helps to bridge the gap of exploring lower cost and available agricultural waste that is not commonly used by researchers for the conduct of agro-runoff wastewaters, such as velvet beans identified as *Mucuna pruriens seed shell* (*MPSS*), that can easily be sourced locally. *MPSS* has been reported to be an effective adsorbent for dyes contaminated wastewater treatment (Igwegbe *et al.* 2016).

Adsorption isotherms are used for the description of how molecules or ions of adsorbate interact with adsorbent surface sites also, critical in optimizing the use of adsorbents (Igwe *et al., 2018)*. The efficacious depiction of the constant change in the surface-assimilative separation of solute from solution on an adsorbent is a good description of the equilibrium separation sandwiched between the two phases (Igwe *et al., 2018)*. Kinetics study is also important for designing sorption systems since swift kinetics generally enable smaller reactors because of the lower retention time for effective adsorbate uptake whereas a slow rate of uptake necessitates series of columns to use the optimum potential of the biosorbent (Igwe *et al.*, 2018, Singh *et al.*, 2021*)*. Hence, this study reports the results of activating the adsorbents and the adsorption of chlorpyrifos on *MPSS*. Effect of adsorbent dosage, contact time, temperature, initial concentration of pesticide, and pH were investigated and adsorption isotherm study was carried out. The kinetics of adsorbate sorption was also used to determine the uptake volume of the sorbent and the rate of uptake of adsorbate by MPSS. The thermodynamics study was also carried out from the results obtained.

2.0 Materials and methods

2.1 Materials and chemicals used

High grade Chlorpyrifos (pesticide) powder, HCL, NaOH, H_3PO_4, distilled water, filter paper and pH of 7 capsules were bought from a standard substance vendor at Onitsha head bridge in Anambra state, Nigeria. The adsorbent (Velvet beans seed) with the botanical name *Mucuna pruriens seeds, locally known as (Okobo)* were purchased from New-market in Enugu state, Nigeria. Figures. 1(a and b) showed *Mucuna pruriens* seed and *Mucuna pruriens* seed shell respectively.

Fig.1a: *Mucuna pruriens seed*

Fig.1 b: *Mucuna pruriens seed shell*

2.2 Preparation of adsorbent

The sample of *Mucuna pruriens shells* was collected and separated from the seed, washed thoroughly, and sundried for 5 hr before being milled with a silver crest Sc-1588 5000W blender. The ground sample was sieved to get the desired particle size (450 μm) and carbonized in a muffle furnace at (350 ^{O}C) for an hour before activating with one mole orthophosphoric acid (H_3PO_4). The impregnation ratio referred to as chemical activation was used in the ratio of 2:1 which is the mass of the activation agent divided by the gathering of adsorbent (Tchatchouang *et al.*, 2022). The impregnation ratio (IR) 2:1 is calculated thus as shown in "Eq. (1)",

$$IR = {}^{VH3PO4}/_{Vmpss} \qquad (1)$$

Where IR stands for impregnation ratio, VH_3PO_4 is volume of orthophosphoric acid and V_{MPSS} represents mass of adsorbent (*MPSS).*

The impregnated sample was stirred at (600 rmp) for 60 min and then allowed for 24 hours after the stirring was repeated before filtering (Uchechuku *et al.*, 2015; Tchatchounang *et al.*, 2022).

The activated sample was carefully washed with distilled water until the desired pH between 6.76 and 7.0 was obtained**.** Then, the sample was dried in a Memmert oven (Din 400050-Ip20) at a moderate temperature of 50 ^{O}C for 30 min and stored in a polythene bag for further use (Igwegbe et al., 2016).

2.3 Preparation of chlorpyrifos

The adsorbate (CLPF) was simulated by dissolving 1g of CLPF powder in 1000 ml of distilled water, the mixture was agitated vigorously for about 3 hr and then kept for 24 hrs to ensure proper dissolution after which the mixture was stirred properly till a homogeneous solution is formed. Hence different concentrations were made ready from the stock solutions (1000 mg/l) to obtain range of initial concentrations (10, 20, 30, 40, 50 and 60) mg/l. This was achieved by measuring out various aliquots (10, 20, 30,40,50 and 60) cm^3 into 1000 cm^3 beakers and made up to the mark with distilled water (Uchechuku *et al.,* 2015). These concentrations were higher than the maximum residual limit (MRLs) of 0.03 mg/l for chlorpyrifos according to (Arain *et al.,*2018). Hence, there is a need for treatment of the contaminated water before discharge into the environment.

2.4 Physicochemical and Instrumental Characterization

Physicochemical properties tell the fitness of an adsorbent for an adsorption procedure (Igwegbe *et al.,*2016; Evwierhoma *et al*., 2018). The physiochemical parameters of *MPSS samples* characterized in this analysis are; moisture and ash content, bulk density, pH, and, surface area using BET with the reference methods are shown in Table 2.4.1 according to (Evwierhoma *et al.,*2018; Mayakaduwa *et al.,* 2015; Obiora-Okafo and Onukwuli., 2018).

2.4.1 Physicochemical Characterization

The physicochemical characterization is shown in the table.

Samples	**Reference method**
Moisture content (%)	Igwegbe *et al*., 2016
Ash content (%)	Igwegbe *et al.* 2016
Bulk density (g/cm^2)	Igwegbe *et al.,*2016
pH	Boadu *et al.*2019
BET Surface area (m^2g^{-1})	Mayakaduwa *et al.,* 2015

2.4.2 Instrumental Characterization

SEM is the technique used to investigate the shape and the surface texture morphology of *MPSS* which promotes binding Yuan *et al*., (2022): EDX plot on the other hand is a plot done before adsorption that displays the elemental composition of *MPSS* such as; carbon, oxygen and then followed by calcium as the major elemental constituents, identified by the sharpness of their peaks: FTIR analysis was used to examine the surface functional groups of the adsorbent (*MPSS)* and to identify those groups such as OH, C-C, O=C=O and Si-O-Si that are responsible for CLPF adsorption: BET is used for analysis of surface area adsorbent (Mayakaduwa *et al.,* 2015). In this study, the BET model version (Asap 2021 V4.02 H)) was used to analyze and determine *MPSS* surface area.

2.5 Experimental procedure

Activated *Mucuna pruriens seed shell* was used as an adsorbent to treat CLPF-contaminated wastewater solution. 250 ml beakers with 100 ml of 30 mg/l CLPF concentration in five different series with *MPSS* (0.5g) dose was set at different temperatures of 27±1ºC, 30ºC, 35ºC, 40ºC, and 45ºC on hot plates with magnetic stirrers. The beakers containing the solute and the solvent were stirred vigorously at 100 rpm speed for 50 min. The reading of the untreated

solute sample which was set at the same wavelength λmax = 505 nm was taken first. At the end of each set time, 10 ml solution is withdrawn and filtered using Whatman filter paper. The filtered samples (treated) absorbance-concentration profile was determined using UV spectrophotometer (model ASUV-6300PC) at λmax = 505 nm according to (Joshi *et al.*, 2023) and the readings taken were recorded in tables. The effects of pH, adsorbent dosage, solute concentration, time, and temperature were studied using the batch adsorption process with a one-factor-at-a-time (OFAT) technique (Igwegbe *et al.*,2016, Igwe *et al.*,2018). For each run, 100 ml of prepared pesticide key sample at pH 6 was treated with 0.5 g of activated (*MPSS*) at a temperature of 27 ±1 ^{O}C for a specific time interval between 10 to 50 min placed on the magnetic hot plate agitated/stirred with a magnetic stirrer at the speed of 100 rpm, at end of each time interval, about 5 ml is filtered out from the sample and, the filtrate analyzed subsequently for residual CLPF concentration using UV/Visible spectrophotometer model ASUV-6300PC, then the amount (q_e) adsorbed per unit mass of adsorbents at the time (t) and the percentage removal of chlorpyrifos is determined using the following Eq. "(2)" and "(3)" according to (Tchatchouang *et al.*, 2022):

$$Qt\left(\frac{mg}{g}\right) = \frac{Co-Ct}{MAC} xVs \quad (2)$$

$$Re\ \% = \frac{co-ce}{co}\ x100 \quad (3)$$

Where C_t, C_o and C_e (mg/l) are the concentrations at a time 't', initial concentration and equilibrium concentration, respectively, Vs is the volume of the solute and MAC is the mass of the adsorbent (Joshi *et al.*,2023). Furthermore, the tentative adsorption data were modelled using the dedicated equations presented in Tables 1, 2 and 3 (Igwegbe *et al.*, 2016, Mayakaduwa *et al*., 2015).

Table 1: Adsorption Isotherm applied in the study (Babadi *et al.*,2018)

Model	Linear equations	Plot made	Parameters calculated	Equation No.
Langmuir	$\frac{c_e}{q_e} = \frac{1}{q_m K_L} + \frac{c_e}{q_m}$	$\frac{c_e}{q_e}\ vs\ c_e$	K_L, q_m, R_L,R^2	(4)
Freundlich	$\ln q_e = \ln k_f + \frac{1}{n}\ln c_e$	$\ln q_e\ vs\ \ln c_e$	K_f, n, R^2	(5)
Temkin	$q_e = \mathrm{B}\ln A + \mathrm{B}\ln c_e$	$q_e\ vs\ \ln c_e$	A,b, R^2	(6)
Halsey	$lnqe = \frac{1}{n4lnKH} - \frac{1}{nHlnqce}$	lnqe vs lnCe	K_H, n_H, R^2	(7)

Where q_e- is the quantity of glyphosate/chlorpyrifos at equilibrium, q_m- maximum Adsorption capacity, K_L- Langmuir isotherm, *R*- universal gas constant, K_f,*n*- Freundlich model constants, *A*,*b*-Temkin constants, K_H, nH – Halsey model constant.

Table 2: Adsorption kinetics models applied (Mahmood *et al*., 2022).

Kinetic mode	Linear Equations	Plots Made	Equation No.
PFO	$\ln(q_e - q_t) = \ln q_e - K_1 t$	$\ln(q_e - q_t)\ vs\ t$	(9)
PSO	$\frac{t}{q_t} = \frac{1}{k_2 q_e^2} + \frac{1}{q_e} t$	$\frac{1}{q_t}\ vs\ t$	(10)
IPD	$q_t = k_{id} t^{1/2} + 1$	$q_t\ vs\ t^{1/2}$	(11)
Elovich	$q_t = E_0 + E_1 \ln(t)$	$q_t\ vs \ln t$	(12)

Where q_e is the Quantity of Glyphosate/ chlorpyrifos rejected at Equilibrium, q_t is the Quantity of Glyphosate/chlorpyrifos rejected at a given time (t), k_1 is pseudo-first order constant, k_2 is pseudo second order constant, k_{id} is intraparticle model constant, E_o and E_1 is Elovich constants.

Table 3: Thermodynamic Equations applied in this study (Joshi *et al.*, 2023)

Thermodynamic mode	Linear Equation	Plot made	Equation No.
Thermodynamics	$ln\ Keq = \frac{\Delta So}{R} - \frac{\Delta Ho}{R} X \frac{1}{T}$	ln Keq vs 1/T	(13)

Where 'T' is temperature, keq- thermodynamic constant.

3.0 Result and Discussion

3.1 The physiochemical properties of adsorbent

The results of the physiochemical properties obtained for *Mucuna pruriens seed shell* is shown in Table 3.

Table 3: Physiochemical properties of the *Mucuna pruriens seed shell*

Samples	MPSS	PMSS
pH	6.7	7.11
Surface area	770.550	768.220
Moisture content %	4.0	2.0
Ash content %	5.6	6.7
Bulk density g/cm^2	0.61	0.71

3.2 Instrumental Characterization Result

3.2.1 SEM characterization of *MPSS* before and after treatment of CLPF and GLYP

The shape and the surface texture morphology of *Mucuna pruriens seed shell* were investigated by SEM technique for *MPSS* before the adsorption of CLPF is shown in Plate 1: (a), (b)and (c). There are pronounced features of an irregular, rough surface with substantial layers of rough heterogeneous pores, cavities and saddles which are favorable properties that increased the adsorption of chlorpyrifos/glyphosate through the active pores on *MPSS* is described in plate 1a and b.

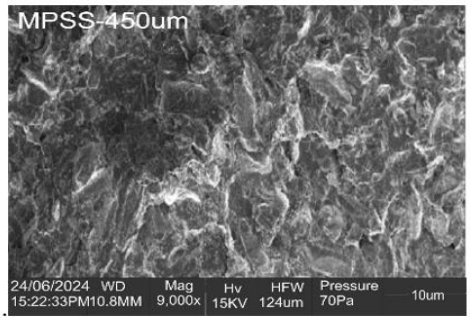

(a) Before adsorption with 10µ

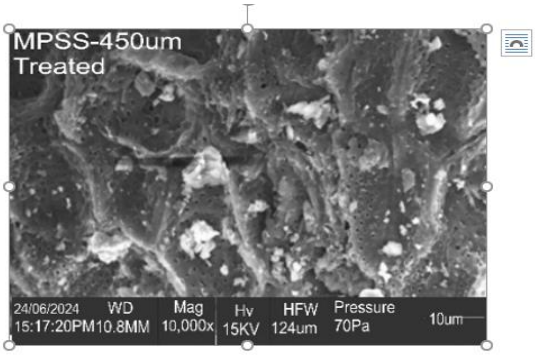

(b) After adsorption with 10µ

Plate 1 a, b: Shape and the surface texture morphology of *Mucuna pruriens seed shell*(10µm) obtained before adsorption(a) and after adsorption (b).

3.2.2 Fourier transform infrared spectroscopy (FTIR) study outcome

FTIR plots of %Transmittance vs wave number for MPSS before activation were presented in Fig. 2.

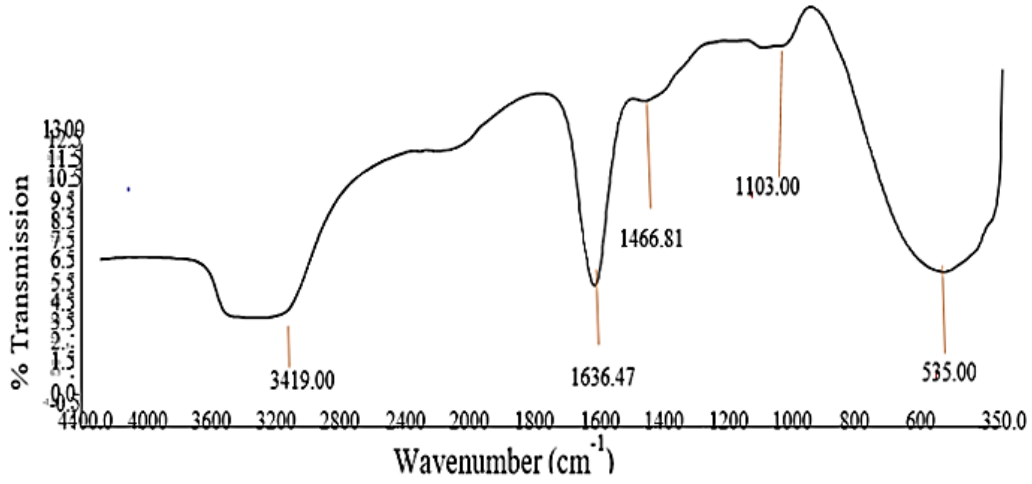

Fig.2: FTIR plots of *MPSS* %Transmittance vs wave number before activation

Peak 3419.00 cm^{-1} showed the presence of strong, broad O−H stretch and H−bend signifying the presence of alcohol and phenol, C=C 1636.47 cm^{-1} widening in alkenyl, medium C−H 1466.81 cm^{-1} bend in alkane, medium bonded C−N 1103.00 extending in aliphatic amines, medium C−Br 1028.00 cm^{-1} widening in alkyl halide.

The FTIR plots of % Transmittance vs wavenumber for *MPSS* after activation as presented in Fig. 3. showed strong peaks at 3690.76 cm^{-1} due to O−H stretching of particle water and ROH at 2930.12 cm^{-1} due to C−H stretching, 2372.33 cm^{-1} C−C stretching in nitriles, 1934 cm^{-1} due to C=C=C stretching, 1826.60 cm^{-1} due to C=O carboxylic acid anhydrides, 759.00 cm^{-1} due to C−H strong aromatics and C−X (haloalkanes) stretching of 686.69 cm^{-1}, 545.00 cm^{-1} and 460.29 cm^{-1} (Babadi *et al*., 2018). Thus, the FTIR spectra show that the surface of *MPSS* after activation contain lots of hydroxyl and carboxylic groups, which perform as proton giver to bind the ions along with the additional medium and weak functional groups participating in the adsorption process (Saga and Isra'a, 2021).

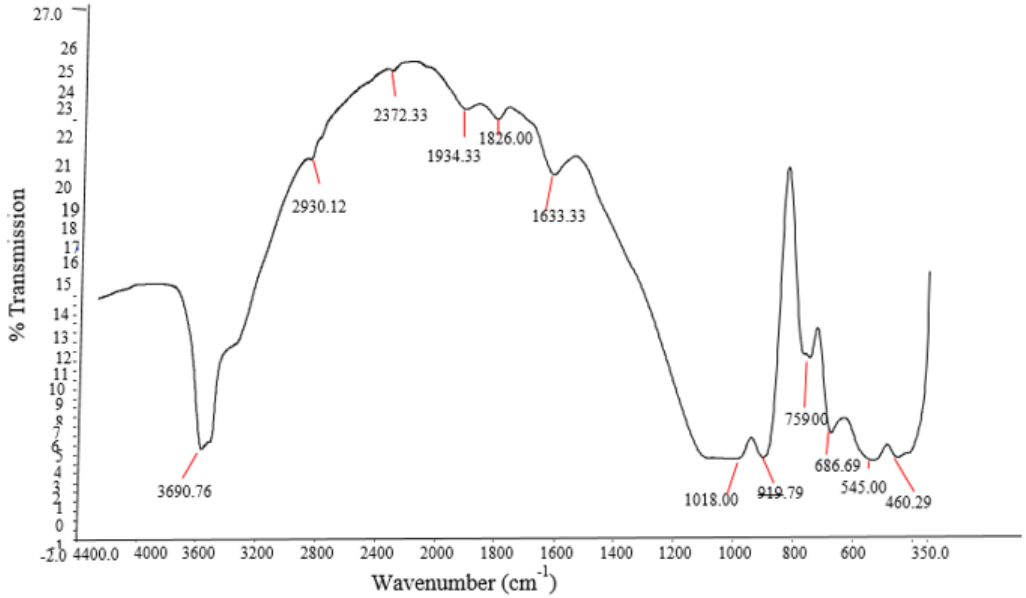

Figure 3: FTIR plot of percentage transmittance of *MPSS* against wavenumber (cm^{-1}) after activation

3.2.3 The BET analysis results

The results of the surface BET surface area before treatment and after are: 770.550 + 3.2220 m^2/g, and 965.450 + 5.2220 m^2/g respectively. This indicates that after activation of *MPSS*, more and larger pores are created hence, a specific surface area, the adsorption collective surface area of pores was between 15.000 m^2/g, 3000.000 m^2/g and, width: 52.330 m^2/g with a total pore volume of 0.584000 cm^3/g, and adsorption average pore width of 27.4400 nm. These results implied that the *MPSS* composite has a high relative high capacity and can accommodate the adsorbed CLPF molecules (Aniagor and Menkiti, 2024). Langmuir correlation coefficient (R^2) of the sorbent was dictated by the BET analysis to be 0.9996000 which agreed with the experimental Langmuir correlation coefficient $R^2 = 0.9995$.

3.3 Batch adsorption capacity

3.3.1 Effect of pH and adsorbent dose on adsorption capacity

CLPF pH was adjusted with either 0.1 mole of NaOH or 0.1 mole of HCl and the pH values range of 2 to 10 were obtained, labelled and placed in a series of 250 ml beakers (Joshi *et al.,* 2023). The investigation was carried out on 100 ml, 30 mg/l of CLPF concentration with 0.5 *g MPSS* at 27±1 ^{O}C, for time intervals of 10 to 50 min, at the end of each set time, about 5 ml of the filtrate was measured out and the absorbance checked in the UV-spectrophotometer the quantity adsorbed is calculated from the calibration curve. The maximum removal of CLPF occurred at optimum pH 6, where 94.23 % was obtained within the first 20 minutes into the process as shown in Fig. 4.

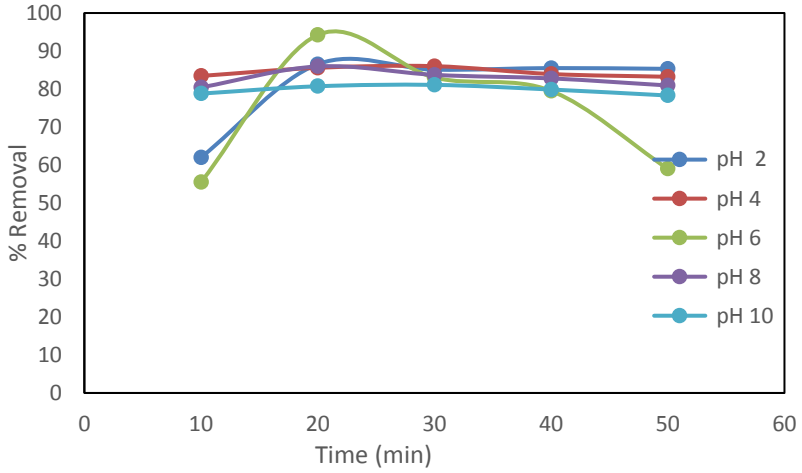

Figure 4: Effect of pH variation vs contact time on the treatment of CLPF onto *MPSS*

It was detected that above pH 6, the percentage removal decreased. The reason could be because chlorpyrifos ions become more negatively charged, resulting in the reduction of adsorption due to repulsion between the anionic ion and the surface layer.

The optimum dose of an adsorbent is a very important factor in the adsorption study since it defines the adsorption capacity of an adsorbent in a given initial concentration (Cara and Jitareanu., 2015). The effects of adsorbent dose on the adsorption of CLPF onto *MPSS* were investigated under controlled conditions, room temperature 27±1 ^{O}C, adsorbate concentration 30 mg/L, pH 6. The experiment was done by altering the dose of adsorbent from (0.3 g to 0.7 g) at different time interval range (10-50 min), the rate of sorption is recorded and the graph of percentage removal against dosage is used to explain the impact of dosage variation as shown in Fig.5.

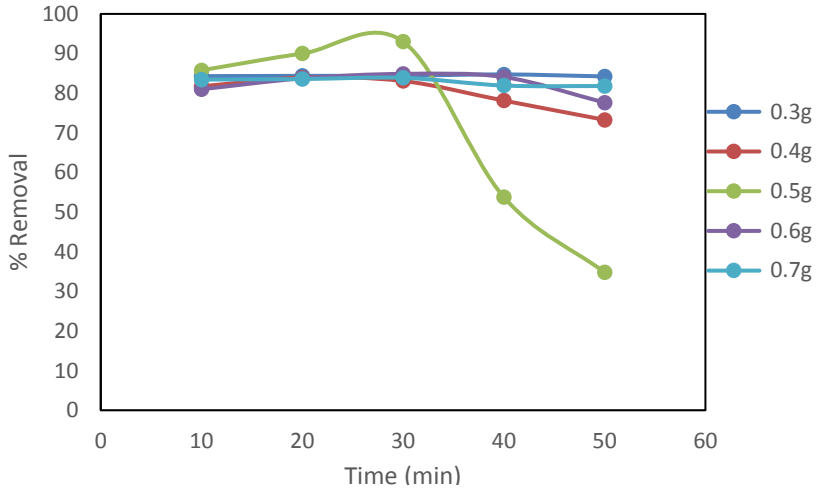

Figure 5: Effect of MPSS dosage on treatment of CLPF

The adsorption percentage rapidly increased as the adsorbent dose was increased above 0.5 g where maximum removal was achieved to be 93% before it dropped. The rise in percentage removal is because an increase in adsorbent dosage increases the number of active sites available for adsorption (Suo et al., 2019b).

3.3.2 Outcome of concentration and time on adsorption capacity

The nature of the adsorption of chlorpyrifos on adsorbent is illustrated in Fig 6.

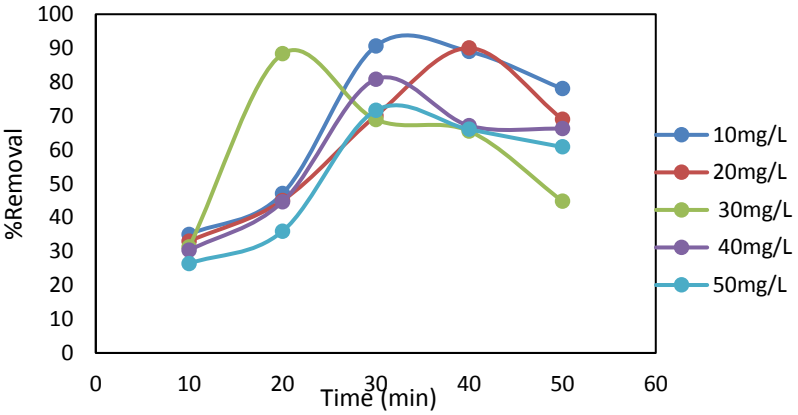

Figure 6: Effect of CLPF initial concentration on MPSS against

As the initial concentration and time changed, readings were taken and percentage removal was plotted against time. It could be seen from the graph that the % removal of CLPF lessened as the initial concentration was increased but, the percentage removal increased with respect to time. The highest percentage removal obtained within the first 30 min of agitation before reaching equilibrium point was above 95 %. Rissoulli *et al.* (2017) obtained similar results with biopolymers as adsorbent for decontamination of water polluted by pesticides using. The root course of reduction in percentage removal could be on the basic fact that the sorption sites were already saturated leaving little or no available sites to accommodate more sorbate molecules, this also suggests that for more proportion removal to be realized within the same period, sorbent dose may be increased. Joshi *et al.*, (2023) reported that the amount adsorbed augmented with increasing sorbate concentration for the adsorption of chlorpyrifos onto boiler fly ash and maize. (Igwe *et al.*,2018) reported that the concentration between adsorbate (chlorpyrifos) on lemon peel in solution (bio adsorbent) surface decrease as time passes. The Temperature variation effect was also studied with temperature variations of 27±1 ^{O}C, 30 ^{O}C, 35 ^{O}C, 40 ^{O}C and 45 ^{O}C under a controlled environment. The percentage yield of activated *MPSS* on CLPF at different temperatures is shown in Fig.7.

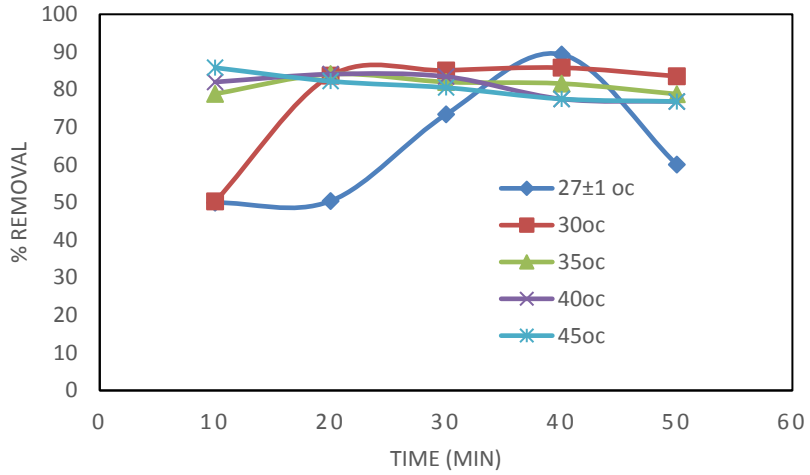

Figure 7: Effect of chlorpyrifos temperature variation on MPSS

where, a maximum percentage removal of above 80 % was realized at room temperatures 27±1 ^{O}C which decreased as temperature increased from (30 - 45) ^{O}C. Joshi et al. (2023) and Igwe *et al.* (2018) got a similar result on the treatment of CLPF with lemon peel and fly ash respectively.

3.4 Isotherm modelling

According to Igwegbe *et al.*, (2016), adsorption isotherm which represents the equilibrium relation between CLPF attention in the fluid phase and that on *MPSS* surface at controlled conditions was examined at room temperature 27±1 ^{O}C, constant pH of 6 using Langmuir, Freundlich, Temkin and Halsey isotherm model. Chlorpyrifos concentration range was 20 mg/l – 40 mg/l. The isotherm plot and model-generated parameter table for CLPF by MPSS; Langmuir, Freundlich, Temkin and Halsey are shown in Figs. 8 – 11 and in Table 4 respectively.

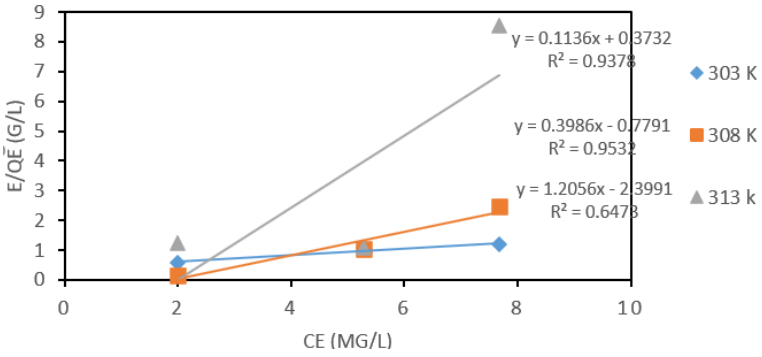

Figure 8: Langmuir isotherm plot

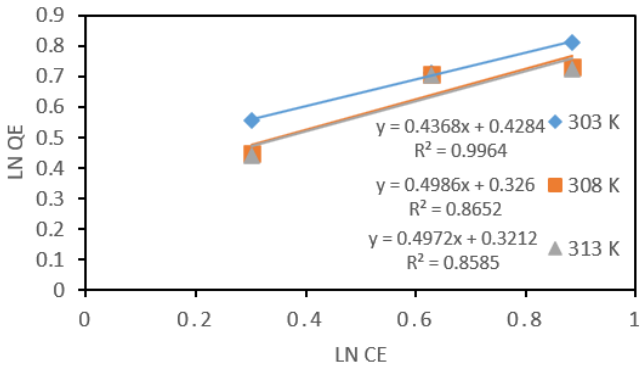

Figure 9: Freundlich isotherm plot

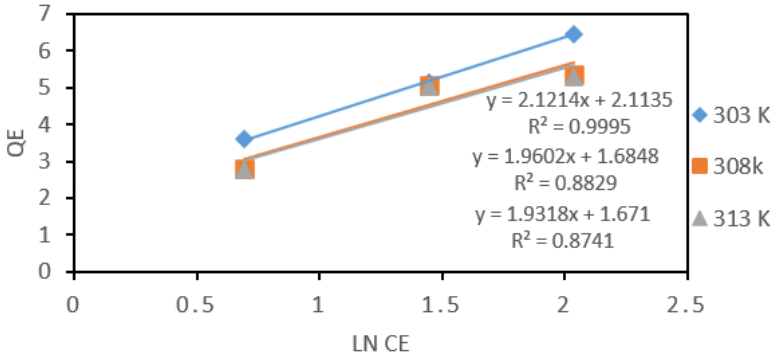

Figure 10: Temkin isotherm model

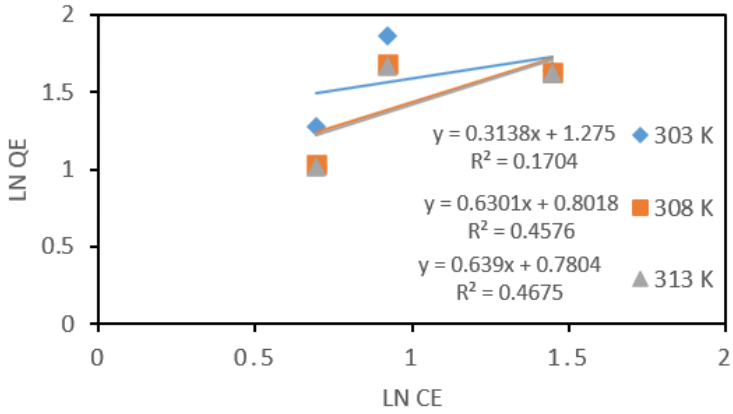

Figure 10: Halsey isotherm model

Q_{max} of 8.8 mg/g was realized and the separation factor (R_L) value (0.0100) was obtained indicating that the adsorption process was favorable and natural at 30 ^{O}C (Igwe *et al.*, 2018). Freundlich model, which supposes multi-layer adsorption and heterogeneous sites, the constant 'n' was 2.2894 and since 'n' > 1but < 10, this simply signifies that the adsorption process is rather physical than chemical. Also, since n values are > 1, invariably, 1/n values are < 1 which is an indication that significant adsorption occurs at low concentrations and the amount of CLPF adsorbed decreased with an increase in attentiveness (Igwe *et* al., 2018). This is the basis for the decrease in CLPF percentage adsorbed in this study from (90.6 – 71.6) % as initial concentrations increased from (10 mg/l – 50 mg/l). From the R^2 > 90 % obtained at 30 ^{O}C, it means that all the models used described the process well except for Halsey isotherm with R^2 < 0.500. However, Temkin gave the highest value of association coefficient R^2> 99.5 %.

Table 4: Isotherm model parameters at initial concentration (20-40) mg/l

Isotherm Model	Temperature		
	303	**313**	**323**
Langmuir			
Q_m (mg/g)	8.80	2.51	0.83
b (L/mg)	3.2852	-1.9576	-1.9899
R_L	0.0100	-0.0173	-0.0170
R^2	0.9378	0.9532	0.6473
Freundlich			
n	2.2894	2.0056	2.0113
K_f (L/g)	2.6816	2.1183	2.0951
R^2	0.9964	0.8652	0.8585
Temkin			
b_T (J/mg)	1,187.49	1306.35	1347.08
A	2.7082	2.3619	2.3749
R^2	0.9995	0.8829	0.8749
Halsey			
K_H	58.154	3.5697	3.3915
n_H	-3.1867	-1.5870	-1.5649
R^2	0.1704	0.4576	0.4675

3.5 Adsorption kinetic studies of chlorpyrifos on MPSS

The kinetic data obtained from the experimental results after treatment of 30 mg/l CLPF solution with 0.5 g *MPSS* at different contact time ranges (10-50) min and temperatures 30 ^{O}C, 35 ^{O}C and 40 ^{O}C were used to predict the behavior of the adsorption process. The kinetic parameters and coefficient (R^2) were lifted from the four different kinetic model plots used to investigate the process which includes; First Order kinetic, Pseudo-first order, Pseudo second order, Elovich and Intraparticle diffusion model order as shown in Figs. 12 – 16 and the data listed in Table 5.

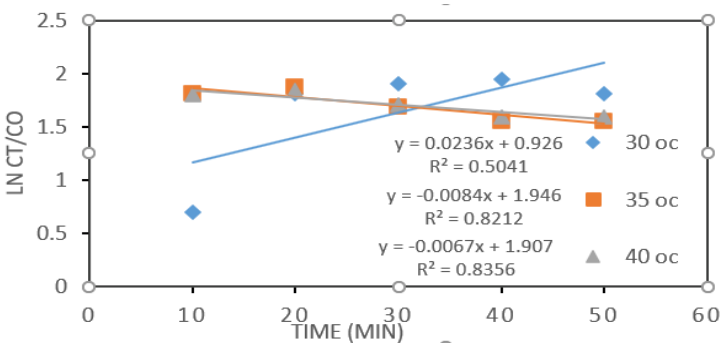

Figure 12: First–Order kinetic plot

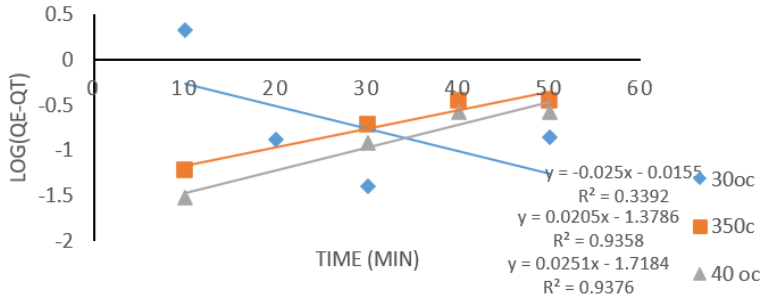

Figure 13: Pseudo-First–Order kinetic plot

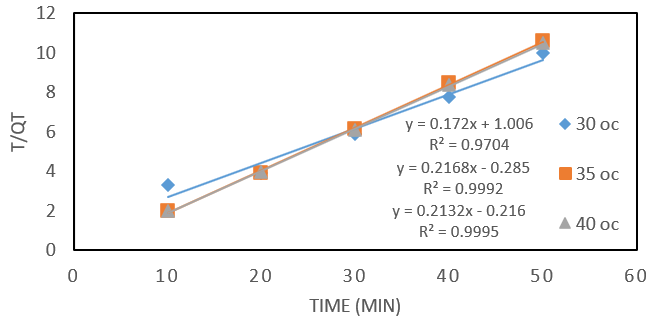

Figure 14: Pseudo-First–Order kinetic plot

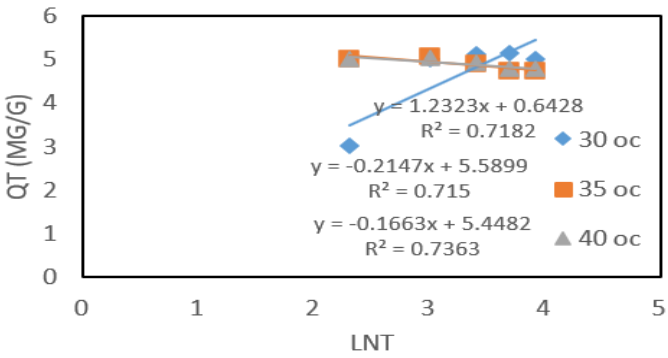

Figure 15: Elovic kinetic plot

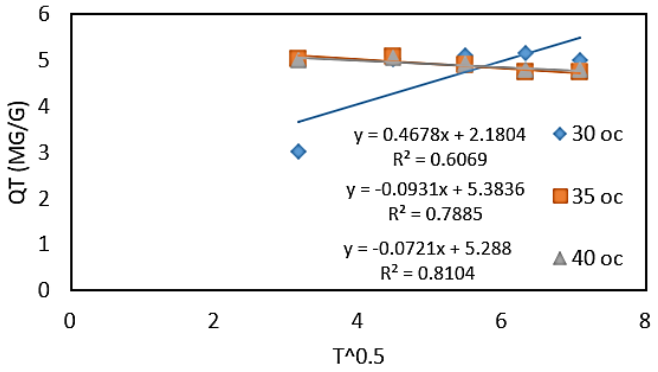

Figure 16: Intraparticle diffusion plot

Table 5: Adsorption kinetics of CLPF onto *MPSS*

Kinetic Model		**Temperature**	
	303	313	323
First order			
K_1 (1/min)	0.0236	0.0084	-0.0067
R^2	0.5042	0.8212	0.8356
Pseudo-first Order			
K_1 (1/min)	0.253x 10^-2	-0.732x10^-2	-2.303x10^-4
q_e (mg g$^-$)	1.644	0.0202	30.123
R^2	0.6889	0.8424	0.3119
Pseudo second Order			
K_1 (g mg^{-1} min^{-1})	0.9940	-3.5088	-4.6298
q_e (mg g$^-$)	+5.8169	+4.6125	+4.6904
R^2	0.9704	0.9992	0.9995
Elovich			
β (g mg^{-1})	+0.8115	-4.6577	-6.0132
Intercept	0.6428	5.5899	5.4482
R^2	0.7182	0.715	0.7363
Intra-particle and film diffusion			
K_{pi} (mg g^{-1}min^{-1})	-0.086	-0.4892	-0.0777
C_i	+2.098	+4.5169	+2.0461
R^2	0.0804	0.8539	0.2876

The top close-fitting kinetic model in this study is pseudo second order (PSO) with a correlation coefficient (R^2) above 97 % at all temperatures. Joshi *et al.*, 2023, obtained similar results on the treatment of chlorpyrifos with lemon peel. The calculated q_e at the temperatures of 30, 35 and 40 ºC were 5.8139 mg/g, 4.6129 mg/g and 4.6904 mg/g respectively. They were all close to the tentative data in the PSO model, thereby validating the model (Babadi *et al.*, 2018). Hence, the best-fit model is PSO kinetics model which described the process's kinetic behavior more accurately than the other four models used.

It was also observed from the values obtained that increase in quantity of chlorpyrifos adsorbed in all the models including PSO model, was not consistent instead of increasing as
the temperature increases, they decreased inconsistently with significant values from each other. This could be because the kinetic complicity of CLPF molecules with the *MPSS* ions in the aqueous phase got distorted by

temperature increase thereby reversing rapidly the entire process. The electrostatic attraction between the ions and the neutral molecules became inert as the temperature exceeded 30 ^{O}C. Therefore, room temperature could be recommended as the most favourable result in this process.

3.6 Thermodynamics Study

Thermodynamic studies carried out in this study disclosed the interaction between *MPSS* and the CLPF, in the form of heat, because of the energy of interaction (Iwuozor *et al.*, 2023). At equilibrium, the Van't Hoff reaction isotherm equation tallies with the free energy (ΔG), standard free energy change (ΔG^0), and the equilibrium constant (K) at room temperature (T) using equation (12) (Aniagor and Menkiti., 2024).

$$\Delta G = \Delta G^0 + RTlnK_e \quad (12)$$

When ΔG become zero, then Eq. (12) changes to Eq. (13)

$$\Delta G^0 = -RTlnK_e \quad (13\,a)$$

or

$$RTlnK_e = -\Delta G^0 \quad (13\,b)$$

Predicting the standard enthalpy change (ΔH°) and standard entropy change (ΔS°), Eq.13 is rearranged into Eq. (14).

$$lnK_e = -\frac{\Delta G^0}{RT} = \frac{\Delta S^0}{R} - \frac{\Delta H^0}{RT} \quad (14)$$

The thermodynamic parameters like; standard free energy change (ΔG^0), enthalpy change (ΔH^0) and enthalpy change (ΔS^0) of the adsorption process were calculated using the experimental data at various temperatures (303 ^{O}K, 308 ^{O}K and 313 ^{O}K). The plot of the thermodynamic study is shown in Fig. 17.

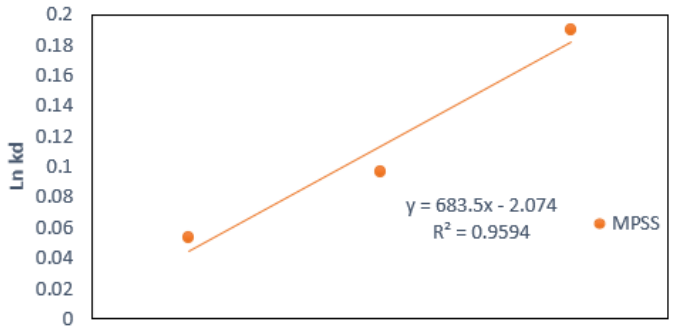

Figure 17: Thermodynamic plot for CLPF on MPSS

The values of ΔG^0 calculated were all positive for the adsorption of CLPF onto *MPSS*, the positive value explained the non-spontaneity of the adsorption process and indicates that it is an ion–dipole and dipole–dipole interaction. The value of ΔG^0, ΔH° and ΔS^0 as shown in Table 6.

Table 6:6 Thermodynamic parameters for CLPF on MPSS

Temp. (k)	ΔG^0	ΔH^0	ΔS^0
303	+0.130	-5.683	-17.243
308	+5.305		
313	+5.391		

The negative ΔH^0 value for the adsorption of CLPF onto *MPSS*, indicates that their process is exothermic and that adsorption activity took place naturally. Joshi *et al.* (2023) obtained a parallel result. The negative value of ΔS° shows decreasing randomness at the adsorption interface. The low enthalpy of the adsorption of chlorpyrifos on *MPSS* indicates a physisorption process.

4.0. Conclusion

This study has revealed that activated *MPSS* could be utilized to remove Chlorpyrifos from the aqueous solution to an appreciable level. Hence, could be recommended as a good bio-adsorbent for agro-runoff treatment. The percentage adsorbed increased with an increase in pH, adsorbent dose, and initial concentration but decreased with an increase in temperature. The equilibrium data was modelled by four isotherm equations but only the Langmuir, Temkin and Freundlich models fitted the adsorption process. However, the Temkin model had the highest correlation coefficient above 99.9% hence, could be described as the best-fitted model for the sorption data at room temperature. For the adsorption kinetics, Pseudo-second order model mostly described the sorption process at all temperatures with R^2 values above 97%. The sorption process was found to follow a physisorption mechanism probably through hydrophobic pesticide-pesticide interactions. In conclusion the present study indicates that *MPSS* could be employed as an adsorbent for the removal of Chlorpyrifos from simulated wastewater.

References

Aniagor, C.O., Menkiti, M.C., 2024. Analysis of metronidazole adsorption onto cellulose-chitosan composite adsorbent. UNIZIK Journal of Engineering and Applied Sciences, 3(5), 1307-1316.

Arain, M., Khan, M.B., Azizullah, C., Rafio, Z.B., Sarmad M., Kundan, K., Abdul, S., 2018. Analysis of Chlorpyrifos Pesticide Residues in Surface Water, Ground Water and Vegetables through Gas Chromatography. Int. Environmental Application and Science, 13(3): 167-173.

Babadi, N., Haman, T., Mozhgan T., 2018. Synthesis and characterization of nanocomposite $NiFe_2$@salenSi and its application in efficient removal of Ni (II) from aqueous solution. Bull. Chem. Soc.Ethiop, 32(1), 77-88. Doi: https://dx.doi.org/10.4314/ bcse. v32il.7.

Badr, S., Isra'a, S., 2021. Using agricultural waste as biosorbent for harzardous brilliant green dyeremoval from aqueous solutions. Journal of Engineering Science and Technology, ER.vl 16.

Boadu, K.O, Joel, O.F, Essumang, D.K, Evbuomwan BO., 2018 Comparative Studies of the Physicochemical Properties and Heavy Metals adsorption

Cara, I.G., Jitareanu, G., 2015. Application of low-cost adsorbents for pesticide removal. Bull. USAMV series Agri. 72 (1), 37e44. https://doi.org/10.15835/.

Dai, Y., Sun, Q., Wang, W., 2018. Utilizations of agricultural waste as adsorbent for the removal of contaminants: A review. Chemosphere 211:235–253. https://doi.org/10.1016/j.chemo sphere.2018.06.179.

EvwierhomaL, E.T., Madubiko, O.D., Jaiyeola, A., 2018. Preparation and characterization of activated carbon from bean husk. Nigerian Journal of Technology (NIJOTECH). 37(3), 674 – 678. http://dx.doi.org/10.4314/njt.v37i3.17.

Ighalo, J.O., Adeniyi, A.G., Oke, E.O., Adewoye, L.T., Motolani, F.O. 2020a. Evaluation of Luffa cylindrica Fibers IN a Biomass packed bed for the treatment of paint industry effluent before Environmental release. Europeon Journal of Sustainable Research, 4(4), emo132.https://doi.org/10.29333/ejosdr/8302.

Igwe, J.C., Okoronkwo, N.E., Eze, S.I., Aghalibe, C.U., 2018. Isotherm and kinetic studies of chlorpyrifos adsorption onto agricultural by products. Chem Res J, 3(5):1–14.

Igwegbe, C.A., Onyechi, P.C., Onukwuli, O.D., Nwokedi, I. C. 2016. Adsorptive Treatment of Textile Wastewater Using Activated Carbon Produced from *Mucuna pruriens* Seed Shells. World Journal of Engineering and Technology, 4,21-37. http://dx.doi.org/10.4236/wjet.2016.41003.

Iwuozor, K.O., Emenike, E.C., Gbadamosi, F.A., Ighalo, J.A., Umenwaeke, G.C., Iwuchukwu, F.E., Nwakire C.O., Igwegbe C.A. 2023. Adsorption of organophosphate from aqueous solution: A review of recent advances. International Journal of Environmental Science and Technology 20;5845-5894.

Joshi, V., Manoj, K.J., Santosh, K.S., 2023. Approaching a discussion on the detachment of chlorpyrifos in contaminated water using different leaves and peels as bio adsorbents. Scientific Reports 13:11186. https://doi.org/10.1038/s41598-023-38471-5.

Kyzas, G.Z., Kostoglou, M. 2014. Green adsorbents for wastewaters: A critical review. Materials (Basel) 7:333–364.

Mahamood, A.V., Varabuntoonvit V.J., Mungkalasiri, T.S., Gheewala S.H., 2022. Absolute environmental sustainability assessment of rice in Pakistan using a planetary boundary-based approach.

Nitin, K.S., Guarav, S., Manish, Y., Hirendrasinh, P., Johnson, C., Vijai, S. 2023. Fate of pesticides in agricultural runoff treatment systems: Occurrence, impacts and technological progress, Environmental Research. Nov 15,237(pt2): 117100.doi: 10.1016/j.envres.2023.117100.PMID:37689336.

Obiora-Okafo, I.A., Onukwuli, O.D. 2018. Characterization and optimization of spectrophotometric colour removal from dye containing wastewater by Coagulation-Flocculation. Polish Journal of Chemical Technology, 20, 4, 49—59, 10.2478/pjct-2018-0054.

Omo-Okoro, P.N., Daso, A.P., Okonkwo, J.O., 2018. A review of the application of agricultural wastes as precursor materials for the adsorption of per- and polyfluoroalkyl substances: A focus on current approaches and methodologies Environ. Technol Innov.

Rahmani, A., Leili, M., Seid-Mohammadi, A., Shabanloo, A., Ansari, A., Nematollahi, D., Alizadeh, S., 2021. Improved degradation of diuron herbicide and pesticide wastewater treatment in a three-dimensional electrochemical reactor equipped with PbO_2 anodes and granular activated carbon particle electrodes. J. Clean. Prod. 322, 129094.

Rissouli, L., Mohamed B., Tarik C., & Mohamed C. 2017. Decontamination of water polluted with pesticide using biopolymers: Adsorption of glyphosate by chitin and chitosan Journal of Materials and Environmental Sciences ISSN: 2028-2508

Saga, B., Samaka, I. 2021., Using agriculturalwaste as biosorbent for hazardous brilliant green dyeremoval from aqueous solutions. Journal of Engineering Science and Technology ER.vl 16.

Singh, T.S., Neha, N., Himanshi, G., Chandra, S.G. 2021., A study on the biosorption kinetics of Cu (II) and Zn (II) ions from aqueous phase (sulphate medium) using sawdust generated from acacia nilotica wood carpentry. 31, 615 – 625, doi: 10:4236/oalib.1103732.

Suo, F., You, X., Ma, Y., Li, Y., 2019. Rapid removal of triazine pesticides by P doped biochar and the adsorption mechanism. Chemosphere. https://doi.org/10.1016/.

Tchatchouang C., Boresse U., Hannah, N. M., Lincold, M. B. Jacques, S. T., Dzoujo T. H., Victor O. S., Achille N. B. & Gerard, P. 2022. Preparation, characterization and application of H_3PO_4-activated carbon from *Pentaclethra macrophylla* pods for the removal of Cr (VI) in aqueous medium. https://doi.org/10.1007/s13738-022-02675-9.

Uchechuku, O.F., Odoemelam S.A., Eddy N.O. 2015. Biosorption of Cd2+, Ni2+ and Pb2+ by the shell of *pentaclethra macrophylla*: equilibrium isotherm studies https://www.journalbinet.com/jstei-volume.

Varsha, J., Jindal, M.K., Sar, S.K., 2023. Approaching a discussion on the detachment of chlorpyrifos in contaminated water using different leaves and peels as bio adsorbents. Scientific Reports. 13:11186.https://doi.org/10.1038/s41598-023-38471-5.

Yuan K., Lingme J., Yuhang X., Jing Z., Jian Z., Xiuyu Y., Guangqiang M., Shuang S. Cheng L., 2022. Facile synthesis and study of functional porous organic polyaminals with ultrahigh adsorption capacity and fast removal rate for rhodamine B dye.

Zalat, O.A., Elsayed, M.S. Fayed, M.K., Abd El, M. 2014. Validation of UV Spectrophotometric and HPLC Methods for Quantitative determination of chlorpyrifos. International Letters of Chemistry, Physics and Astronomy (2) 58-63 ISSN 2299-3843.